St. Joseph's Journal of Humanities and Science
ISSN: 2347 - 5331
http://sjctnc.edu.in/6107-2/

Structural, Vibrational, Morphological and Magnetic Properties of Copper Ferrite Nano Particles ($Cu_{0.4M}Fe_{2.96M}O_4$) by Co-precipitation Method

R. Sagayaraj*
H. Jude Leonard Hilary
S. Xavier
P. Praveen
K. Elayakumar
C. Yogambal

ABSTRACT

The copper ferrite nanoparticles (NPs) have been prepared by the co-precipitation method. The crystal structure, crystallite size, surface morphology and magnetic properties were analysed using various technique tools to exhibit the formation of the inverse spinel structure, surface nature and their magnetic behaviour respectively. The XRD analysis shows the single phase of the proposed material without any impurities. FT-IR spectra confirmed the formation of the $CuFe_2O_4$ nanoparticles and displayed clear transmittance peaks at ~ 545 and 470cm^{-1} which are characteristic for the spinel crystal structure. The FESEM shows prickly pear cactus shaped morphology, when the sample annealed at 900°C. The VSM reveals that the proposed material exhibited the super paramagnetic nature.

Keywords: Copper ferrite, Polycrystalline, Absorption, Morphology, Super paramagnetic.

INTRODUCTION

Copper ferrite have been widely used for many optoelectronic devices, catalysis, gas sensor, optical switch, magnetic storage media, energy storage, solar energy transformation, field emission device, lithium ion batteries, High-density magneto-optic, recording devices, color imaging, bioprocessing, magnetic refrigeration and ferrofluids, magnetic cores, optomagnetic devices, bubble memory devices [1-5]. Gennerly, The spinel ferrite is formulated by MFe_2O_4, where M is the divalent metal ion. The crystal lattice of the stable low-temperature phase of $CuFe_2O_4$ exhibit a tetragonal distortion, mainly due to the Jahn–Teller effect of $Cu^{(II)}$ cations [6,7]; As-deposited room temperature copper ferrite

PG and Research Department of Physics, St. Joseph's College of Arts and Science (Autonomous), Cuddalore-607001, Tamil Nadu, India.
*E-Mail: sagayarajnancy@gmail.com.

thin film was tetrahedral crystal structure (due to Jahn-Teller distortion of Cu^{2+} ion at octahedral site), showing the properties comparable to that of bulk material after annealing [8], and above 900°C is cubic . Tetragonal $CuFe_2O_4$ is an inverse spinel in which $Cu^{(II)}$ cations occupy mainly octahedral B-sites, whereas $Fe^{(III)}$ cations are found on B-sites and tetrahedral A-sites with approximate equal occupancy[9-10]. The lattice parameter determined for the $CuFe_2O_4$ is 8.374 A°. This value of the lattice parameter is closer to the values: 8.370 A° (JCPDS 77-0010) corresponding to the inverse spinel structure (Fe^{3+}) $A(Cu^{2+}Fe^{3+})BO_4$, according to Verwey and Heilmann and 8.382 A° (JCPDS 75-1517) which correspond to a partially inverse spinel structure [10]. In addition, copper ferrites with body-centered tetragonal crystal structure phase (JCPDS 34-425) were formed. This structure was confirmed with the peaks appearing at ''d'' values of 2.583 and 2.056 A° On increasing firing temperature to 1000°C, the peaks characterized for both iron oxide and copper oxide almost disappeared and only copper ferrite peaks with tetragonal structure were present. Two interesting observations could be deduced on further increasing the firing temperature to 1100°C. The first was the change in the crystal structure of the formed copper ferrites from body-centered tetragonal to cubic structure (JCPDS 77-0010). This change was illustrated by the appearance of peaks at ''d'' values of 2.0929 and 1.4817 A°, which characterized the cubic phase of copper ferrites [12]. FT-IR absorbance spectrum for CuO nanoparticles at different Fe molar ratios, many trials have been done to confirm them using the Peak Fit computer program, at last it was found that the Gaussian band is the best fit. The results confirmed that pure CuO phase had three broad absorption peaks at 582, 535 and 489 cm-1, assigned to the stretching vibrations of Cu-O bond in the monoclinic Cuo. Generally for spinel ferrite, the band υ1 around 600 cm^{-1} was belonging to stretching vibration of tetrahedral complexes and υ_2 around 400 cm^{-1} was related to that of octahedral complexes. It can be seen that the observed band at 585 cm^{-1} in the spectrum of $CuFe_2O_4$ was attributed to the stretching vibration of tetrahedral coordinated Fe- O bonds [1, 5]

EXPERIMENTAL DETAILS

Materials

Copper (II) sulfatepenthydrate ($CuSO_4.5H_2O$ assay:98%),Ferric sulfate monohydrate ($Fe_2(SO_4)_3.H_2O$, assay: 99), Ethanol(C_2H_5OH), Ammonia(NH_3), polyvinyl pyrrolidone $(C_6H_9NO)n$, were purchased from Sigma Aldrich. All chemical was used without any further purification.

Synthesis of PVP coated $Cu_{0.4M}Fe_{2.96M}O_4$ nanoscale particles

The ferrite ($Cu_{0.4M}Fe_{2.96M}O_4$) has been prepared by the co-precipitation technique. Stoichiometric amount of Ferric sulfate monohydrate ($Fe_2(SO_4)_3.H_2O$: 2.96M),), Copper (II) sulfate pentahydrate($CuSO_4.5H_2O$: 0.04M), polyvinyl pyrrolidone (PVP:1g) and Ammonia (NH_3=0.025M) were dissolved in distilled water to got a mixed solution. The molar ratio of ferric sulfate to copper sulfate was 1:2 the mixed solution was placed on hot plate under vigorously stirring. Finally, the prepared NH_3 solution was added drop wise to the above solution under continuous stirring for 3hrs at 50°C, which serve as a precipitator. Then the precipitator materials were centrifuged and it washed several times by deionized water. After drying samples were annealed at 900°C.

CHARACTERIZATION

The $Cu_{0.4M}Fe_{2.96M}O_4$ ferrite powder were subjected to XRD analyses with(LabX XRD-6000) with CuKα radiations to analyze the structural parameters. FT-IR (Jasco 660+) in KBr disc has been used to determine the structure formation. The morphology of materials were characterized by scanning electron microscopy SEM(JEOL JEM-3010 SEM).

XRD analysis

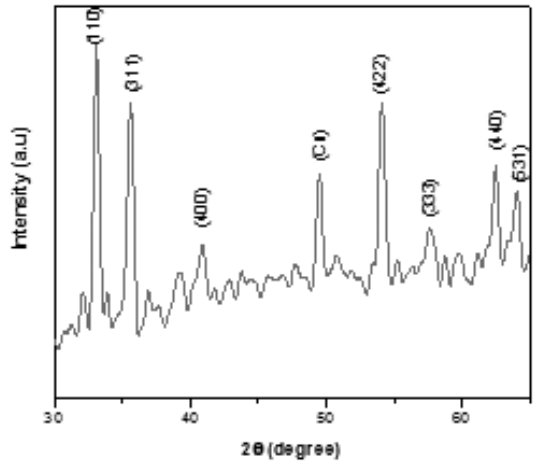

Fig.1. X-ray Diffraction of $Cu_{0.04M}$ $Fe_{2.96M}O_4$ Nanoparticles

Fig. 1 shows the XRD patterns of $Cu_{0.4M}Fe_{2.96M}O_4$ samples were annealed at 900°C. Using XRD results, crystallite size was calculated by using Debye-Scherer equation[13],

$$C_s = 0.9 \lambda / \beta \cos \theta$$

Here, C_s stands for crystallite size; λ is the wavelength the radiation and β is the full width half maximum (in radians), and θ is the corresponding angle of diffraction. The calculated size of the crystallite is 4.2 nm. From the XRD pattern the hkl parameters were identifiedas(110),(311),(400),(422),(333),(440),(531), and they are matched with standard JCPDS data Card No: 89-4307. The copper ferrite exhibited the single phase of the proposed material without any impurities [10].In fact that the replacement of Fe^{2+}/Fe^{3+} cations by Cu^{2+}cations led to crystallite size due to ionic radius (Cu^{2+}:0.72A; Fe^{2+}: 77 pm; Fe^{3+}: 63 pm). Consider the electronic configuration of Fe^{2+}[Ar] $3d^6$ and Fe^{3+}[Ar] $3d^5$ (For comparison, Fe [Ar] $4s^2$ $3d^6$). Fe^{3+} ionic radius is 63 pm, while Fe^{2+} has an ionic radius of 77 pm. (For comparison, the Fe atom has a radius of 140 pm). This is because the outermost electron in the Fe^{2+} ion is pulled off to form Fe^{3+} ion. As the electrons are removed, it reduces the repulsion increasing nuclear charge experienced by each of the other d electrons and decreases the size of the ion. The lattice constant of the copper ferrite was calculated by the following relations [18, 19],

$$a = [d^2 (h^2+K^2+l^2)]^{1/2}$$

'a' lattice constant deal with a physical dimension of all crystal system and magnetic materials structure. The lattice constant of copper ferrite is ~8.34A°. It is revealed that the Shape of a nanoparticle exhibit the cubic structure because of lattice constant as reported for pure copper ferrite [10].

FT-IR analysis

FT-IR spectra can offered information about coordination / distribution of cations between octahedral and tetrahedral site. FT-IR spectra was recorded from the range of 400-4000 cm^{-1} and it shown in Fig. 2. Generally, for spinel ferrite, the band (υ_1) around 545 cm^{-1} was belonging to stretching vibration of tetrahedral complexes (Fe^{3+}-O^{2-}) and (υ_2) around 470cm^{-1} was related to that of octahedral complexes (Cu^{2+}- O^{2-}.The intensities of transmitted band at 976cm^{-1} , 1111 cm^{-1} are the characteristics of copper ferrite system because of remaining FeOOH system [1,13,14], revealing to the formation of a spinel structure for $CuFe_2O_4$. At 1629 cm^{-1} assigned to the stretching (υ) vibrations of the free or absorbed water on the surface of Iron–copper ferrite nanoparticles [15, 16]. The O–H stretching vibrations interacting through H bonds are observed at 3191 cm^{-1}.

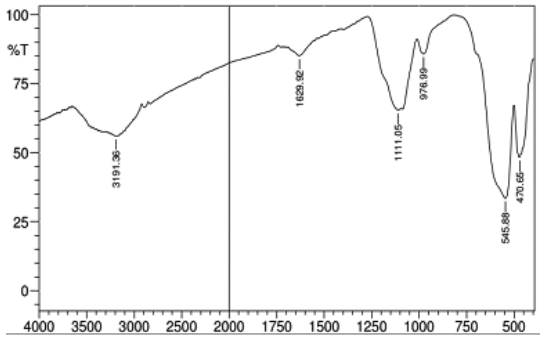

Fig.2 .FTIR Spectra of Cupper ferrite nanoparticles of $Cu_{0.04M}$ $Fe_{2.96M}O_4$

The variations observed in the positions of ν_1 and ν_2 by changing the method and conditions of the preparation are attributed to the shifting of Fe^{3+} and Cu^{2+} ions towards O^{2-} occupied tetrahedral and octahedral sites [4].

FESEM analysis

FE-SEM technique was used to analyze the surface nature of the prepared material and it displayed in Fig. 3. The sample was annealed at 900°C condition

based ferrite powders were revealed the prickly pear cactus nature. This morphology should be attributed to the higher temperature of synthesis which allows the grain growth and a reduction of porosity [9]. The surface morphology of copper ferrite nanoparticles at pH = 8, annealed at 900°C. It shows the agglomerated flaky and sponge like particles [13]. Therefore, the growth and densification of smaller ferrite nanoparticles were higher than larger ferrite nanoparticles. The smaller nanoparticles have higher surface energy, and consequently, a higher driving force for grain growth and densification to reduce the system's Gibbs energy [20].

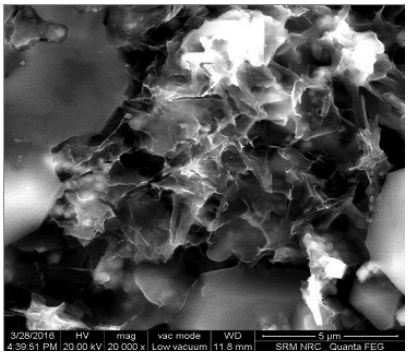

Figure 3: SEM images of $Cu_{0.04M}Fe_{2.96M}O_4$ nanoparticles

VSM ANALYSIS

The magnetic parameters depend on several parameters e.g. the cation distribution between octahedral and tetrahedral sites, the cation super exchange interactions and grain size [4]. On the other hand, the electronic 8 configurations of Cu^{+2} and Fe^{+3} ions were $3d^9$ and $3d^5$ whereas the magnetic moments of Cu^{+2} and Fe^{+3} ions were 1.73 and 5.9 μB, respectively in the high spin state. Subsequently, the magnetic moments of Fe ions were larger than Cu ions. The incorporation of Fe in CuO lattice enhances the magnetic moment. Consequently, the overall total magnetic moment was increased [1, 12]. In such a case, some Cu^{2+} ions occupy (A) site, which diminishes the tetragonal distortion. This causes a drastic change in its magnetic response by doubling the effective magnetic moment per unit formula and decreases its crystalline anisotropy. This phenomenon could be attributed to the fact that the ideal configuration of tetrahedral copper ferrite consists of eight divalent (Cu^{2+}) ions on the octahedral (B) sites and 16 trivalent (Fe^{3+}) ions equally splitting between the tetrahedral (A) and (B) sites per unit cell. The magnetization of the (A) sublattice is antiparallel to that of the (B) sublattice, whereas the magnetic moments of the ions on the (A) and (B) sublattices are ferromagnetically ordered. The total magnetic moment of copper ferrite is entirely due to the uncompensated magnetic moment of the eight Cu^{2+} ions on the (B) sites. The saturation magnetization and the coercive field Hc of the pure copper oxide sample annealed at 600°C for 1h were 0.10 emu/g and 136.93 Oe, respectively reported by M.M. Rashad et al. [1]. As can be seen, the mesoporous samples have a crystalline form with the mean dimensions in the range of 6.57-8.27 nm and a magnetic core with smaller dimensions. This implies the magnetic core of particles is surrounded by a disordered surface layer, forming magnetic core-shell nanoparticles repotted by Najmeh Najmoddin et al [17] .The Ms value of 27.09 emu/g found for Cusolid (particle size of 36 nm) was as good as to the value of 33 emu/g for $CuFe_2O_4$ nanoparticles of ~32 nm data carried out by S. S. Selima et al [5].

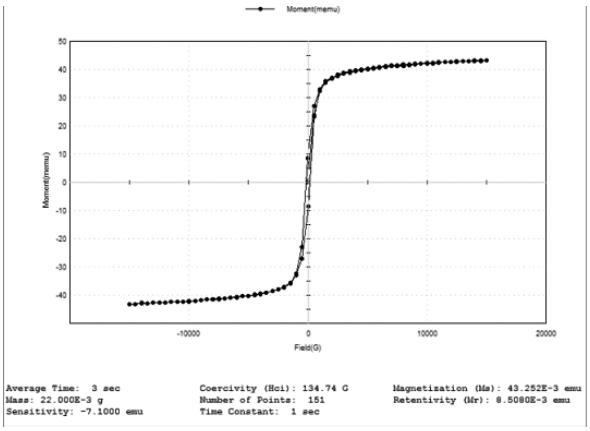

Figure 4: VSM image $Cu_{0.04M}Fe_{2.96M}O_4$, nanoparticles at room temperature

The magnetic curve of copper ferrite ($Cu_{0.4M}Fe_{2.96M}O_4$) as showed in the Fig 4, which reveals the lesser loop area and illustrated super paramagnetic properties. The saturation magnetization (Ms) value of nanoparticle for sample is 43E-3emu/g, coercive field be the 134.74G, ramanance ratio is 0.196 and magnetic moment be the 1.9×10-3 μB. The super paramagnetic performance of these materials indicates a great promise of their use as materials for magnetic resonance imaging (MRI) application.

CONCLUSION

The copper ferrites were successfully synthesized by a co-precipitation method. Using XRD analysis the formation of the spinel structure has been confirmed. FT-IR spectra confirmed the M-O vibrating band through the tetrahedral and octahedral site coordination with oxygen ions. The FE-SEM, image prickly pear cactus nature, when the sample was annealed at 900 °C. Super paramagnetic nature was studied at room temperature measurements using the VSM analysis.

ACKNOWLEDGEMENT

We remain grateful to the Management of St. Joseph's College of Arts & Science (Autonomous), Cuddalore, Tamil Nadu, India, for the funding under the scheme Intramural Research Projects 2017-2018 (SJC/IP/2017-18/02) and for permitting to use the facility of a research lab for "Nanotechnology and Crystal growth"

REFERENCES

1. M.M. Rashad, S. Soltan, A.A. Ramadan, M.F. Bekheet, D.A. Rayan, Ceramics International 41(2015) 12237-12245
2. C.D.Lokhande, Journal of Magnetism and Magnetic Materials 313 (2007) 69–75
3. A.T. Raghavender , Nguyen Hoa Hong , Chulkwon Park , Myung-Hwa Jung ,Kyu Joon Lee , Daesu Lee, Journal of Magnetism and Magnetic Materials 324 (2012) 1814 –1817
4. S.S. Selima, M. Khairy, M.A. Mousa, Ceramic International,45 (2019) 6535-6540.
5. S. Anandan, T. Selvamani, G.Guru Prasad, A. M. Asiri, J. J. Wu, Journal of Magnetism and Magnetic Materials 432(2017)437-443,
6. Mrugesh Desai, Shiva Prasad, N. Venkataramani, Indradev Samajdar,A.K. Nigam, R. Krishnan, Journal of Magnetism and Magnetic Materials 246 (2002) 266–269
7. A .M. Balagurov , I.A. Bobrikov , V. Yu. Pomjakushin , D.V. Sheptyakov ,V. Yu. Yushankhai, Journal of Magnetism and Magnetic Materials 374 (2015) 591 –599
8. C.D. Lokhandea,b, S.S. Kulkarnia, R.S. Maneb, Sung-Hwan Han, Journal of Magnetism and Magnetic Materials. 313 (2007) 69–75
9. Julia E. Tasca , Claudia E. Quincoces , Araceli Lavat , Ana M. Alvarez , M. Gloria Gonza´lez, Ceramics International. 37 (2011) 803–812
10. T.F. Marinca , I. Chicinas, O. Isnard, Ceramics International. 38 (2012) 1951–1957
11. M. Kuc˘era, , V. Kolinsky´ , S. Vis˘n˘ ovsky´ , D. Chvostova´ , N. Venkataramani, S. Prasad, P.D. Kulkarnic, R. Krishnan, Journal of Magnetism and Magnetic Materials 316 (2007) 688–691.
12. Y.M.Z. Ahmed, M.M. Hessien, M.M. Rashad, I.A. Ibrahim, Journal of Magnetism and Magnetic Materials 321 (2009) 181–187
13. S. Pavithradevi, N. Suriyanarayanan, T. Boobalan, Journal of Magnetism and Magnetic Materials 426 (2017)137-143,
14. Naghikhani, R., Nabiyouni, G. & Ghanbari, D. J Mater Sci: Mater Electron (2018) 29: 4689.
15. J. Balavijayalak shmi, N. Suriyanarayanan , R. Jayaprakash,Journal of Magnetism and Magnetic Materials 385 (2015) 302–307
16. Ghassemi, N., Davarani, S.S.H. & Moazami, H.R. J Mater Sci: Mater Electron (2018) 29: 12573.
17. Najmeh Najmoddin, Ali Beitollahi, Hüseyin Kavas, Seyed Majid Mohseni, Hamidreza Rezaie, Johan Åkerman, Muhammet S. Toprak,Ceramics, International 40(2014) 3619-3625
18. R. Sagayaraj • S. Aravazhi • P. Praveen • G. Chandrasekaran, Journal of materials science: materials in electronics 29 (2018)
19. R. Sagayaraj • S. Aravazhi • G. Chandrasekaran, Journal of Superconductivity and Novel Magnetism 31 (2018) 603
20. Nanhua Wu, Xiaoyan Ji, Wenlong Xie, Chang Liu, Xin Feng, and Xiaohua Lu, Langmuir, 33 (2017) 11719-11726